PCCP

Accepted Manuscript

ROYAL SOCIETY OF CHEMISTRY

www.rsc.org/pccp

PCCP

RSCPublishing

ARTICLE

Decomposition of fluorophosphoryl diazide: A joint experimental and theoretical study†

Cite this: DOI: 10.1039/x0xx00000x

Dingqing Li,[a] Hongmin Li,[a] Bifeng Zhu,[a] Xiaoqing Zeng,*[a] Helge Willner,[b] Helmut Beckers,*[c] Patrik Neuhaus,[d] Dirk Grote[d] and Wolfram Sander[d]

Received 00th January 2014,
Accepted 00th January 2014

DOI: 10.1039/x0xx00000x

www.rsc.org/

The photolytic and thermal decomposition of fluorophosphoryl diazide, $FP(O)(N_3)_2$, was studied by matrix isolation spectroscopy. Upon ArF laser photolysis (λ = 193 nm), FPO and a new germinal azido nitrene $FP(O)(N_3)N$ were identified by matrix IR spectroscopy. The nitrene shows a triplet ground state with the zero-field parameters $|D/hc|$ = 1.566 cm^{-1} and $|E/hc|$ = 0.005 cm^{-1}. Further decomposition of the nitrene into FPO was observed under irradiation of λ > 335 nm. In contrast, no nitrene but only FPO was identified after flash vacuum pyrolysis of the diazide. To reveal the decomposition mechanism, quantum chemical calculations on the potential energy surface (PES) of the diazide using DFT methods were performed. On the singlet PES four conformers of the nitrene were predicted. The two conformers (*syn* and *anti*) showing intramolecular $N_{nitrene}\cdots N_{\alpha,azide}$ interactions are much lower in energy (ca. 40 kJ mol^{-1}, B3LYP/6-311+G(3df)) than the other two exhibiting $N_{nitrene}\cdots O$ interactions. *Syn/anti* refers to the relative orientation of the P=O bond and the N_3 group. The interconversion of these species and the decomposition into FPO via a novel three-membered ring diazo intermediate *cyclo*-$FP(O)N_2$ were computationally explored. The calculated low dissociation barrier of 45 kJ mol^{-1} (B3LYP/6-311+G(3df)) of this cyclic intermediate rationalizes why it could not be detected in our experiments.

Introduction

Nitrene intermediates play an important role in organic synthesis and biology.[1–2] Photolytic or thermal decomposition of covalent azides are general methods for producing highly reactive nitrenes by releasing molecular nitrogen. The formation and reactions of nitrenes have attracted extensive theoretical and experimental studies in the past few decades.[3–6]

The electronic properties of nitrenes largely depend on substitution. The parent nitrene HN and simple alkyl nitrenes (RN) have triplet ground states, where two unpaired electrons are localized on the hypovalent nitrene center. Large singlet-triplet energy gaps (ΔE_{ST}) were estimated for these nitrenes by calculations.[7–8] However, in carbonyl nitrenes (RC(O)N) the ΔE_{ST} values become relatively smaller, and in some cases a singlet ground state has been suggested by quantum chemical calculations and proved by experimental observations.[9] Such a significant electronic change was rationalized by an intramolecular interaction between the nitrene center and the adjacent oxygen atom ($N_{nitrene}\cdots O$), which stabilizes the close-shell singlet by forming a cyclic oxazirine-like structure (Scheme 1).[10–15]

Such intramolecular interactions have also been proposed for the related singlet α-oxo nitrene intermediates $R_2P(O)N$[16–18] and $RS(O)_2N$.[19–22] Even though, a triplet ground state has recently been confirmed for the sulfonyl and phosphoryl nitrenes, $FS(O)_2N$[19–20] and $F_2P(O)N$,[16] by matrix-isolation spectroscopy (IR, UV/Vis, and EPR), these oxo nitrenes are liable to an exceptional photo-induced oxygen-shift isomerization from $X_nE(O)N$ to X_nENO (X_nE = F(O)S and F_2P). It has been concluded that such a unique oxygen-shift Curtius-rearrangement will be facilitated by significant intramolecular $N_{nitrene}\cdots O$ interactions in their lowest-lying singlet excited state (Scheme 1).[16, 19–20]

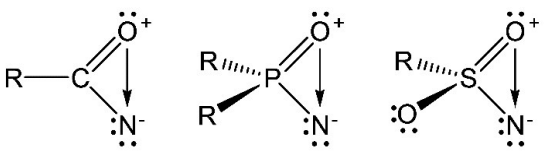

Scheme 1 Intramolecular O→N interactions in singlet α-oxo nitrenes.

Apart from nitrenes, decomposition of covalent polyazides was utilized to produce some long-sought species.[23–24] The presence of an azide group in the initially generated nitrenes may alter their electronic properties due to the lone-pair electrons on the nitrogen atom at the α position of the azide group. This might provide access to some synthetically difficult molecules. One recent example is the synthesis of diazirinone (*cyclo*-N_2CO) via pyrolysis of carbonyl diazide ($OC(N_3)_2$),[25–26] where the germinal azido nitrene ($N_3C(O)N$) was proposed to be involved as an

intermediate (Scheme 2).[27] Although the intriguing reaction mechanism for the formation of *cyclo*-N_2CO from $N_3C(O)N$ has not yet been revealed, the possible formation of novel small-ring systems from germinal diazides stimulates us to extend our studies to the photolytic and thermal decomposition of other main-group covalent azides.

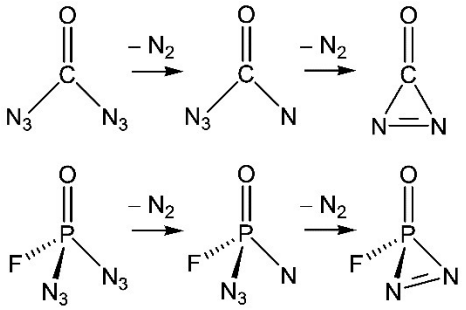

Scheme 2 Possible decomposition pathways for $OC(N_3)_2$[27] and $FP(O)(N_3)_2$.

In this work, we have studied the photolytic and thermal decomposition of fluorophosphoryl diazide, $FP(O)(N_3)_2$, by matrix isolation spectroscopy. This diazide is of particular interest in view of the present study, since a stepwise N_2 elimination might provide access to two metastable intermediates, the geminal azido phosphorylnitrene $FP(O)(N_3)N$, and the cyclic phosphadiazirine derivative $FP(O)N_2$ (Scheme 2). Furthermore, the azido phosphorylnitrene might be stabilized by two competing intramolecular interactions to the hypovalent nitrene center, involving either the polar phosphoryl oxygen or the lone-pair electrons on the α-nitrogen atom of the azido ligand.

Experimental methods

Caution! Covalent azides are in general explosive. Although no explosion was encountered with $FP(O)(N_3)_2$ during this work, it should be handled with care in millimolar quantities (< 5 mmol) and appropriate safety precautions should be taken.

Sample preparation

Fluorophosphoryl diazide, $FP(O)(N_3)_2$, was prepared by the reaction of $F_2P(O)Cl$ with NaN_3 and purified according to literature.[28] For the preparation of a ^{15}N-labeled sample, 1-^{15}N sodium azide (98 atom % ^{15}N, EURISO-TOP GmbH) was used as received. For the preparation of an ^{18}O-labeled sample, ^{18}O-enriched $F_2P(O)Cl$ (95 atom % ^{18}O) was used.[16] The purity of the samples were checked by IR spectroscopy.

Matrix IR spectroscopy

Matrix-IR spectra were recorded on a FT-IR spectrometer in a reflectance mode using a transfer optic. A KBr beam splitter and an MCT detector were used in the spectral region of 4000–550 cm^{-1}. A Ge-coated 6 μm Mylar beam splitter combined with a liquid helium-cooled Si bolometer and a CsI window at the cryostat were used in the region of 700 to 200 cm^{-1}. For each spectrum, 200 scans at a resolution of 0.25 cm^{-1} were co-added. Gaseous $FP(O)(N_3)_2$ was mixed with argon (1:1000) in a 1-L stainless-steel container and then small amounts (ca. 1 mmol) of the mixture were directed through an aluminium oxide furnace and deposited within 30 minutes onto the cold matrix support (16 K, Rh-plated Cu block) in a high vacuum. Details of the matrix apparatus have been described elsewhere.[29]

Matrix EPR spectroscopy

For electron paramagnetic resonance (EPR) measurements, the matrices were deposited on an oxygen-free high-conductivity copper rod (75 mm in length, 3 mm in diameter) that was cooled by a Sumitomo SHI-4-5 closed-cycle 4.2-K cryostat. The vacuum system consisted of a vacuum shroud equipped with a sample inlet valve and a half-closed quartz tube (75 mm length, 10 mm diameter) at the bottom, and a vacuum-pump system with a Pfeiffer Vacuum TMU071P turbo pump backed by a Leybold two-stage, rotary-vane pump. During deposition, the inlet port was positioned at the same height as the tip of the copper rod, and for the measurement of EPR spectra the entire apparatus was moved downwards so that the quartz tube and copper rod were positioned inside the EPR cavity. X-band EPR spectra were recorded with a Bruker Elexsys E500 ESR spectrometer equipped with an ER077R magnet (75 mm pole cap distance), and an ER047 XG-T microwave bridge. Computer simulation of EPR spectra were performed using the XSOPHE computer simulation software suite (version 1.0.4),[30] developed by the Centre for Magnetic Resonance and Department of Mathematics, University of Queensland, Brisbane (Australia) and Bruker Analytik GmbH, Rheinstetten (Germany).

Flash vacuum pyrolysis and photolysis

Small amounts of the argon diluted (1:1000) sample were passed through an aluminium oxide furnace (i.d. 1.0 mm, o.d. 2.8 mm, length 25 mm), which was heated (voltage 5.6 V, current 2.0 A) to about 1000 ℃ over a length of ca. 10 mm with a tantalum wire (o.d. 0.25 mm, resistance 1.0 Ω). The residence time in the hot zone is estimated to be in the order of a few milliseconds. Laser photolysis was carried out using an ArF excimer laser (Lambda-Physik, 2 mJ, 5 Hz). UV/Vis irradiations were performed with a high-pressure mercury lamp (TQ 150, Heraeus) by passing the light through water-cooled quartz lenses combined with cutoff filters (Schott).

Computational details

Structural optimizations were performed using density functional theory (DFT) methods of B3LYP,[31] BP86,[32] MPW1PW91.[33] The basis set of 6-311+G(3df) was employed throughout. The complete basis set method (CBS-QB3)[34] was also used for the calculation of relative energies. Local minima were confirmed by vibrational frequency analysis, and transition states by additional intrinsic reaction coordinate (IRC) calculations.[35–36] All calculations were performed using the Gaussian 03 software package.[37]

Results and discussion

Photolysis of $FP(O)(N_3)_2$ in solid argon

As has been shown in our recent studies, short-pulsed (5 Hz) ArF laser photolysis of matrix-isolated azides is a very useful method for generating highly reactive nitrene intermediates in solid noble gas matrices, e.g., $F_2P(O)N$,[16] $FC(O)N$,[14] and $FS(O)_2N$.[19] Similarly, $FP(O)(N_3)_2$ shows a strong UV absorption at about 200 nm, which allows its photolysis by an ArF excimer laser (λ = 193 nm). The IR difference spectrum after photolysis, showing the depletion of the precursor and formation of new species upon photolysis, is depicted in Figure 1 (upper trace).

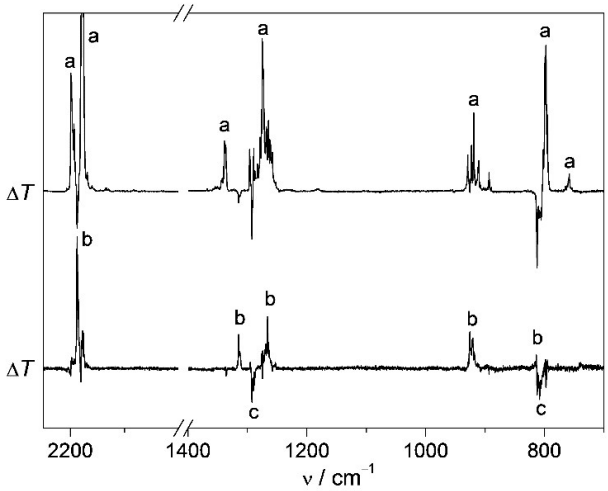

Fig. 1 IR difference spectra (transmission, *T*) of Ar-matrix isolated $FP(O)(N_3)_2$ at 16 K. Upper trace: after ArF laser irradiation (λ = 193 nm). Lower trace: after subsequent near-UV visible irradiation (λ > 335 nm). Bands of depleted species point upward, while bands of newly formed species point downward. Bands associated with $FP(O)(N_3)_2$ (**a**), $FP(O)(N_3)N$ (**b**), and FPO (**c**) are marked.

Clearly, a few new bands appear immediately upon photolysis. The intensities of the two strongest bands at 1292.5 and 812.5 cm^{-1} increase steadily with the time of photolysis, they are in good agreement with the reported frequencies of ν(PO) = 1292.2 cm^{-1} and ν(PF) = 811.4 cm^{-1} for triatomic species FPO,[38] indicating a complete decomposition of $FP(O)(N_3)_2$ upon the laser photolysis. Interestingly, a few new weak bands were also observed, especially a strong one at 2187.5 cm^{-1}, which occurred right between the two bands for the N_3 antisymmetric stretches the diazide precursor (2199.5 and 2178.3 cm^{-1}).

To identify these weak bands, subsequent irradiation using near-UV visible light (λ > 335 nm) was applied to the matrix-isolated photolysis products. The resulting IR difference spectrum is shown in Figure 1 (lower trace). Some weak bands together with the strongest one at 2187.5 cm^{-1} vanished completely, whereas the bands of the diazide precursor were not affected by the irradiation. As can be seen in the spectrum (Figure 1, lower trace), the carrier of these bands exclusively produces FPO upon > 335 nm photolysis. Attempts to increase the yield of this intermediate by prolonged laser photolysis were unsuccessful due to its simultaneous decomposition into FPO. In addition to the band at 2187.5 cm^{-1}, three weaker absorptions at 1315.1, 1266.1, and 923.6 cm^{-1} can be unambiguously identified. Interestingly, these band positions are very close to those of the diazide precursor ($\nu_{as}(N_3)$: 2199.5 and 2178.3 cm^{-1}, ν(PO): 1338.7 cm^{-1}, $\nu_s(N_3)$: 1274.9 cm^{-1}, and ν(PF): 919.1 cm^{-1}, which strongly suggest the formation of the nitrene $FP(O)(N_3)N$ after loss one of N_2 molecule from the diazide.

Calculations on $FP(O)(N_3)N$ were performed for the lowest energy singlet and triplet states (Table 1). Generally, the observed band positions and relative intensities are in better agreement with calculations for the triplet ground state (vide infra). With the aid of calculations, weaker bands in the far-infrared region recorded with a liquid He cooled Bolometer detector could also be identified (Fig. S1, ESI‡). Photolysis experiments were also performed using ^{18}O and ^{15}N enriched $FP(O)(N_3)_2$ (IR difference spectra are shown in Fig. S1-S2, ESI‡). The ^{18}O isotopic shifts for ν_7 ($\Delta\nu_{exptl}$ = 1.1 cm^{-1}, $\Delta\nu_{calcd}$ = 1.2 cm^{-1}), ν_9 ($\Delta\nu_{exptl}$ = 6.1 cm^{-1}, $\Delta\nu_{calcd}$ = 6.6 cm^{-1}), ν_{10} ($\Delta\nu_{exptl}$ = 6.7 cm^{-1}, $\Delta\nu_{calcd}$ = 7.2 cm^{-1}), and ν_{11} ($\Delta\nu_{exptl}$ = 1.8 cm^{-1}, $\Delta\nu_{calcd}$ = 2.2 cm^{-1}) strongly support the assignment to the nitrene $FP(O)(N_3)N$ in its triplet state. As for the ^{15}N enriched sample, the assignment of ^{15}N isotopic shifts were difficult due to the presence of several isotopomers in the matrix. The ^{15}N experiment confirms the assignment of the band at 1315.1 cm^{-1} to ν(PO) since no ^{15}N isotopic shift was observed for this band.

Table 1. Calculated and experimental vibrational frequencies (cm^{-1}) and intensities of triplet $FP(O)(N_3)N$

experimental[a]	calculated[b]		assignment[c]
Ar-matrix	*syn*	*anti*	
2187.4 s	2305 (552)	2296 (551)	ν_1, $\nu_{as}(N_3)$
1315.1 ms	1302 (124)	1321 (61)	ν_2, ν(PO)
1266.1 ms	1352 (272)	1345 (379)	ν_3, $\nu_s(N_3)$
923.6 ms	901 (194)	867 (150)	ν_4, ν(PF)
813.9 w	796 (67)	790 (67)	ν_5, ν_{as}(NPN)
739.6 vw	726 (26)	717 (16)	ν_6, ν_s(NPN)
582.7 w	592 (48)	591 (41)	ν_7, $\delta_{i.p.}(N_3)$
	579 (5)	579 (14)	ν_8, $\delta_{o.o.p.}(N_3)$
455.5 w	427 (40)	422 (40)	ν_9
404.1 w	400 (34)	385 (31)	ν_{10}
363.8 vw	352 (10)	369 (14)	ν_{11}
	268 (4)	266 (3)	ν_{12}
	243 (2)	246 (3)	ν_{13}
	133 (1)	128 (1)	ν_{14}
	57 (< 1)	55 (< 1)	ν_{15}

[a] Experimentally observed frequencies and relative band intensities: s strong, ms medium strong, w weak, vw very weak. [b] Calculated IR frequencies and intensities (km mol^{-1}) in parenthesis at the B3LYP/6-311+G(3df) level of theory. [c] Assignments are given for the *syn* conformer (i.p. in plane, o.o.p. out of plane)

To determine the nature of the electronic ground state of the nitrene intermediate, a matrix EPR spectrum was recorded of the products obtained by ArF excimer laser photolysis of $FP(O)(N_3)_2$ at 5 K. A weak but distinct signal showing characteristic triplet nitrene nature was found (Fig. S3, ESI‡). The derived zero-field parameters at g = 2.0023, are $|D/hc|$ = 1.566 cm^{-1} and $|E/hc|$ = 0.005 cm^{-1}. These are fairly close to those of related triplet phosphoryl nitrenes $F_2P(O)N$ ($|D/hc|$ = 1.60 cm^{-1} and $|E/hc|$ = 0.0054 cm^{-1})[16] and $(PhO)_2P(O)N$ ($|D/hc|$ = 1.5408 cm^{-1} and $|E/hc|$ = 0.00739 cm^{-1}).[39]

Flash vacuum pyrolysis of $FP(O)(N_3)_2$

Flash vacuum pyrolysis of $FP(O)(N_3)_2$ diluted with argon (1:1000) was applied at about 1000 ℃ and the products were subsequently trapped at 16 K (Figure 2, upper trace).

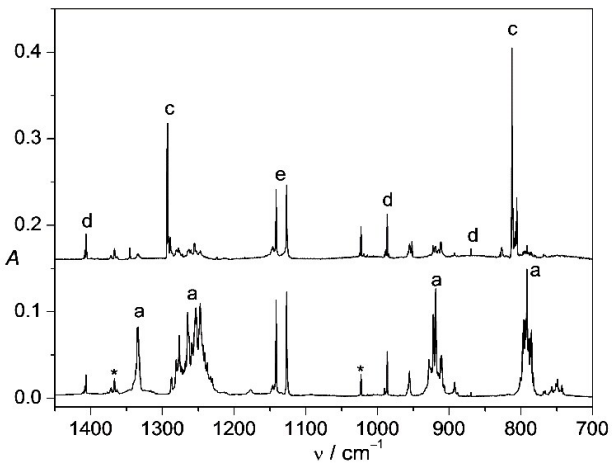

Fig. 2 IR spectra (Absorption, *A*) of Ar-matrix isolated ^{15}N-labeled $FP(O)(N_3)_2$ before (lower trace) and after flash vacuum pyrolysis (upper trace) at 16 K. Bands of $FP(O)(N_3)_2$ (a), FPO (c), F_3PO (d), and HN_3 (e) are marked, bands of unknown impurities are marked by asterisks.

The strong IR bands at 1293.2 and 812.4 cm^{-1} assigned to FPO clearly demonstrate the decomposition of $FP(O)(N_3)_2$. The frequencies of these bands are slightly shifted compared to those observed after photolysis of the diazide, due to the different local matrix environment. Traces of the precursor still survived the pyrolysis, as evidenced by weak IR bands of the diazide (Figure 2, lower trace). The byproducts HN_3 and F_3PO were identified with the aid of ^{15}N labeling. These side products are likely formed by traces of moisture. To identify weak IR bands of photolabile intermediates, the matrix-isolated pyrolysis products were irradiated with λ > 395 nm light. However, no change was found in the IR spectra. Thus, flash vacuum pyrolysis of $FP(O)(N_3)_2$ offers an efficient way of producing FPO in the gas phase, which was formerly generated by either high-temperature reaction of $P(O)FBr_2$ with silver,[38] electric discharge of a $PF_3/O_2/Ne$,[40] or flash vacuum pyrolysis of F_2POPF_2.[41]

Conformers of $FP(O)(N_3)N$

Calculations on the structures and energies of the nitrene $FP(O)(N_3)N$ in both its singlet and triplet states were performed using various DFT methods (B3LYP, BP86, and MPW1PW91). Since the complete basis set method CBS-QB3 was found to give better estimation of the singlet-triplet energy gaps (ΔE_{ST}) of nitrene intermediates,[9,17] it was also applied to $FP(O)(N_3)N$. Optimized structures are shown in Figure 3. Their relative energies are compiled in Table 2. Consistent with experimental EPR observations, a triplet ground state is conclusively predicted by all applied methods. For the most stable conformers on the triplet and singlet hypersurfaces ΔE_{ST} = 35.2 kJ mol^{-1} (CBS-QB3). This is substantially smaller than those of $F_2P(O)N$ (83.5 kJ mol^{-1})[16] and $(CH_3)_2P(O)N$ (65.7 kJ mol^{-1})[17] at the same theoretical level.

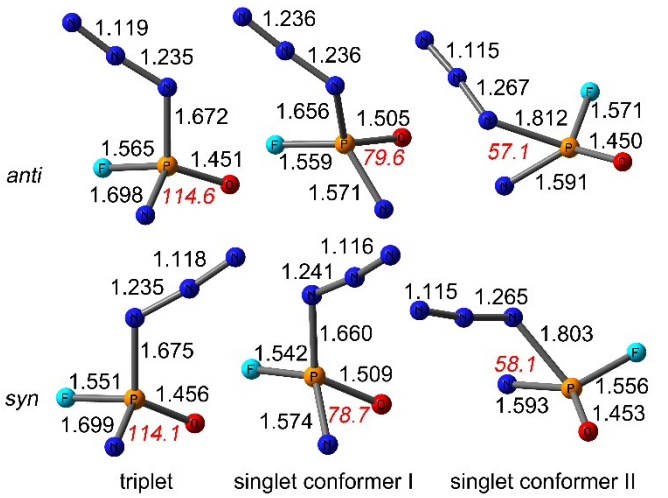

Fig. 3 Calculated conformers of $FP(O)(N_3)N$ in the triplet and singlet states at the B3LYP/6-311+G(3df) level of theory. Selected bond lengths (Å) and selected angles (°, red italics) are also shown. Nitrogen, oxygen, fluorine, and phosphorus atoms are shown in blue, red, cyan, and orange color, respectively.

Two conformers, *syn* and *anti*, were predicted for both triplet and singlet $FP(O)(N_3)N$ (Figure 3), where *syn*/*anti* refers to the relative orientation of the P=O and N_3 moieties with respect to the P–N_α bridge. In both states, *syn* is slightly lower in energy than *anti* (Table 2). A preference of the *syn* conformation has also been found in $F_2P(O)N_3$, which was rationalized by anomeric interaction from the nitrogen lone-pair (N_α) to the $\sigma^*(P{=}O)$.[42]

Table 2. Calculated relative energies (kJ mol^{-1}) of FP(O)(N_3)N

methods	triplet[b]		singlet[b]			
	syn	*anti*	*syn*-I	*syn*-II	*anti*-I	*anti*-II
B3LYP[a]	0.0	5.6	91.4	55.9	100.7	56.7
BP86[a]	0.0	4.4	64.4	22.3	72.3	23.9
MPW1PW91[a]	0.0	5.9	102.7	58.3	113.1	59.2
CBS-QB3	0.0	6.6	69.6	35.2	82.0	37.0

[a] Basis set of 6-311+G(3df) was used. [b] Structures of the conformers are given in Figure 3.

For the lowest singlet state two different *syn* and *anti* conformers were found (conformer I and conformer II in Figure 3). The most striking structural differences between these conformers are related to $N_{nitrene}\cdots O$ (conformer I) versus $N_{nitrene}\cdots N_\alpha$ intramolecular interactions (conformer II): small ∠OPN angles in I (*syn* 78.7, *anti* 79.6 °), whereas even smaller ∠N_αPN angles were found in II (*syn* 58.1, *anti* 57.1 °). Conformers II are lower in energy (Table 2), and the global minimum on the singlet PES is *syn*–II, which corresponds to the smallest ΔE_{ST} of 35.2 kJ mol^{-1} at the CBS-QB3 level.

The rather strong $N_{nitrene}\cdots N_\alpha$ intramolecular interactions in II, is also evidenced by the N_α–N bond lengths of 1.662 and 1.639 Å in *syn*-II and *anti*- II, respectively, which indicate three membered ring N_α-P-N structures. As expected, the ∠OPN and ∠N_αPN angles of the conformers in the triplet ground state are fairly close to a tetrahedral coordination at phosphorus, and there are no indications for such intramolecular interactions in the triplet ground state.

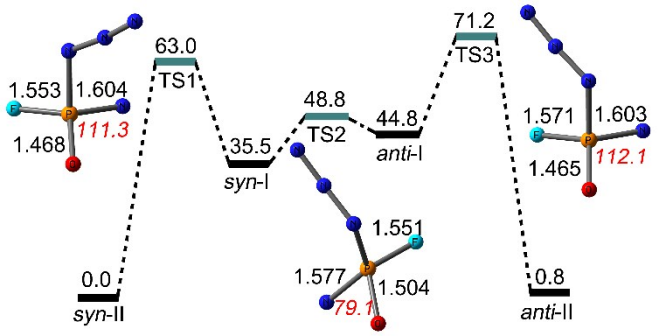

Fig. 4 Inter-conversion of FP(O)(N_3)N conformers on the singlet PES at the B3LYP/6-311+G(3df) level of theory. Relative energies are given in kJ mol^{-1}, selected bond lengths (Å) and angles (°, red italics) are also shown. Nitrogen, oxygen, fluorine, and phosphorus atoms are shown in blue, red, cyan, and orange color, respectively.

To gain insight into the photochemistry of Ar-matrix isolated FP(O)(N_3)N the inter-conversion of its four conformers on the singlet PES was explored at the B3LYP/6-311+G(3df) level of theory (Figure 4). Transition states (TS) for the II to I rearrangements for both the *syn* (TS1) and the *anti* (TS3) configurations were located at activation energies of 63.0 and 70.4 kJ mol^{-1}, respectively. The displacement vectors of the imaginary frequencies of TS1 and TS3 mainly correspond to the NPN$_\alpha$ bending mode. The barrier for the *syn*-I to *anti*-I conversion (TS2) is much lower and was calculated to be 48.8 kJ mol^{-1}. The corresponding displacement vector of the imaginary frequency mainly corresponds to a rotation of the azide group around the P–N_α bond. However, the analogous direct *syn*-II to *anti*-II rearrangement is precluded by the strong $N_{nitrene}\cdots N_\alpha$ interaction, which prevents the free rotation of the azide group.

A singlet phosphoryl nitrene intermediate (Ph_2P(O)N) has been very recently detected by ultra-fast spectroscopy,[43] and its life-time has been estimated to be about 480 ps. Given the low I to II conversion barriers, and the expected rapid singlet-triplet intersystem crossing (ISC) in solid Ar matrixes aided by the small ΔE_{ST} (Table 2), the detection of the most stable triplet nitrene conformer in a solid argon matrix is reasonable. Nonetheless, the absence of FP(O)(N_3)N in the flash pyrolysis products, and the almost exclusive formation of FPO prompted us to investigate also competing secondary reactions of singlet FP(O)(N_3)N such as rapid N_2 elimination or its Curtius-type rearrangement.

Formation and decomposition of *cyclo*-FP(O)N_2

Rather low activation barriers (< 10 kJ mol^{-1}) for the elimination of N_2 from *syn*-II and *anti*-II were predicted on the singlet PES (TS4 and TS5, Figure 5 and Figure S4, ESI‡). These barriers are significantly lower than those predicted for the stepwise N_2 elimination in the phosphoryl azides $(CH_3)_2$P(O)N_3 (189.2 kJ mol^{-1}) and $(CH_3O)_2$P(O)N_3 (174.6 kJ mol^{-1}).[17] As the common decomposition product, a novel three-membered ring molecule *cyclo*-FP(O)N_2 is predicted from FP(O)(N_3)N (Figure 5).

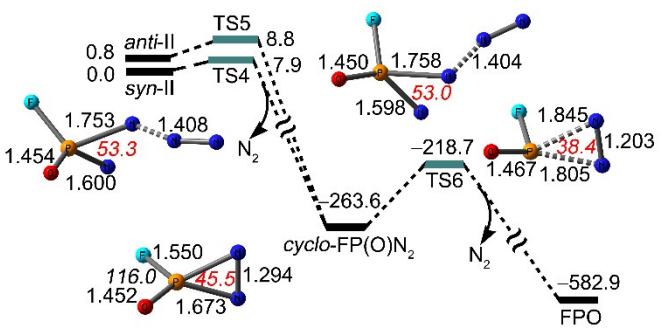

Fig. 5 Calculated decomposition routes for two FP(O)(N_3)N conformers at the B3LYP/6-311+G(3df) level of theory. Relative energies are given in kJ mol^{-1}, selected bond lengths (Å) and angles (°, red italics) are also shown. Nitrogen, oxygen, fluorine, and phosphorus atoms are shown in blue, red, cyan, and orange color, respectively.

The decomposition barrier of *cyclo*-FP(O)N_2 was calculated to be merely 44.9 kJ mol^{-1}, which is much lower than that of *cyclo*-N_2CO (103.1 kJ mol^{-1}) calculated at the same level of theory. The latter compound has been very recently isolated as a neat substance and found to have a half-life time of 30 h at room temperature in a clean quartz container.[26] The main difference

for the decomposition mechanisms of these two cyclic diazo molecules is that the two P–N bonds in *cyclo*-FP(O)N_2 break simultaneously, while the two C–N bond undergo stepwise cleavage in *cyclo*-N_2CO to yield an open-chain isomer OCNN, which undergoes further decomposition to CO and N_2 without barrier on the singlet PES.[44–45] The low decomposition barrier of *cyclo*-FP(O)N_2 probably accounts for its absence among the flash vacuum pyrolysis products, where only its decomposition product FPO was detected by IR spectroscopy.

Decomposition of FP(O)N_4

A Curtius-type rearrangement has recently experimentally been observed for $(N_3)_2$P(O)N.[23] The high energy compound N_3P(O)N_4 was formed under visible light irradiation of the nitrene.[23] However, all attempts to locate transition states for the N_3-migration in singlet FP(O)(N_3)N failed, and only the aforementioned TS1 and TS3 leading to the cyclic minima *syn*-II and *anti*-II (Figure 4) were obtained. This result is consistent with the experimental observation that no rearrangement product but only FPO was found upon near-UV visible light irradiation (λ > 335 nm).

Nevertheless, molecular structures and decomposition pathways of the possible rearrangement product FP(O)N_4 were calculated. Two planar conformers, *cis* and *trans*, were found, which are close in energy and they differ mainly in the configuration (*cis* or *trans*) of the P=O and the N_α–N_β bonds with respect to the P–N_α bridge (Figure 6). The transition states, TS7 and TS8, leading to the concerted decomposition of *cis* and *trans* FP(O)N_4 into FPO + 2 N_2 were located at activation energies of 39.1 and 39.0 kJ mol^{-1}, respectively. With an energy release of more than 500 kJ mol^{-1} these fragmentation reactions of FP(O)N_4 are highly exothermic.

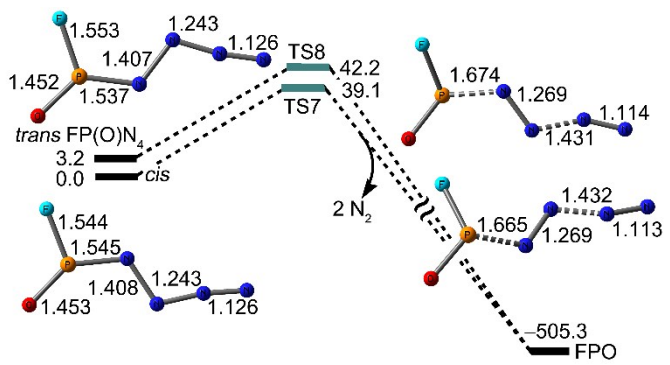

Fig. 6 Calculated decomposition routes for two FP(O)N_4 conformers at the B3LYP/6-311+G(3df) level of theory. Relative energies are given in kJ mol^{-1}, selected bond lengths (Å) are also shown. Nitrogen, oxygen, fluorine, and phosphorus atoms are shown in blue, red, cyan, and orange color, respectively.

Conclusions

Both photolytic and thermal decomposition reactions of FP(O)$(N_3)_2$ were studied by matrix isolation. Upon ArF laser photolysis (λ = 193 nm), a new triplet α-oxo nitrene intermediate, FP(O)(N_3)N, was produced and characterized by matrix IR and EPR spectroscopy. Further decomposition of this nitrene into FPO was observed under near-UV visible irradiation (λ > 335 nm). In contrast, flash vacuum pyrolysis of FP(O)$(N_3)_2$ exclusively yields FPO, and no intermediate species was found. Different decomposition pathways of FP(O)(N_3)N were theoretically explored on the singlet PES. The cyclic conformers *syn*-II and *anti*-II (Figure 3), stabilized by intramolecular $N_{nitrene}\cdots N_{\alpha,azide}$ interactions, were found to be much lower in energy than *syn*-I and *anti*-I (Figure 3), stabilized by intramolecular $N_{nitrene}\cdots O$ interactions. According to DFT calculations singlet FP(O)(N_3)N decomposes by stepwise N_2 elimination to yield FPO via *cyclo*-FP(O)N_2. The low computed activation barrier of 44.9 kJ mol^{-1} (B3LYP/6-311+G(3df)) for the decomposition of *cyclo*-FP(O)N_2 to FPO and N_2, however, rules out its experimental observation in the flash pyrolysis products of FP(O)$(N_3)_2$.

Acknowledgements

This research was supported in part by the National Natural Science Foundation of China (21372173, 21422304), the Project of Scientific and Technologic Infrastructure of Suzhou (SZS201207), the Priority Academic Program Development of Jiangsu Higher Education Institutions (PAPD), and the Deutsche Forschungsgemeinschaft (WI 663/26-1). X.Q.Z. greatly appreciates Professor H. Willner for a research stay in his lab. We are indebted to T. Benter and his group to make use of the ArF laser.

Notes and references

[a] College of Chemistry, Chemical Engineering and Materials Science, Soochow University, 215123 Suzhou, China. E-mail: xqzeng@suda.edu.cn
[b] FB C-Anorganische Chemie, Bergische Universität Wuppertal, 42119 Wuppertal, Germany.
[c] Institut für Chemie und Biochemie, Freie Universität Berlin, 14195 Berlin, Germany. E-mail: beckers@zedat.fu-berlin.de
[d] Lehrstuhl für Organische Chemie II, Ruhr-Universität Bochum, 44780 Bochum, Germany.

† Electronic Supplementary Information (ESI) available: Observed matrix IR and EPR spectra, calculated vibrational displacement vectors for the imaginary frequencies of the transition states, and atomic coordinates for all species discussed. See DOI: 10.1039/b000000x/

1 M. S. Platz, *Reactive Intermediate Chemistry*, Wiley-Interscience, New York, 2004.
2 W. Lwowski, *Azides and Nitrenes*, Academic Press, New York, 1984.
3 S. Bräse, C. Gil, K. Knepper and V. Zimmermann, *Angew. Chem., Int. Ed.* 2005, **44**, 5188.

4 S. Lang and J. A. Murphy, *Chem. Soc. Rev.*, 2006, **35**, 146.
5 N. P. Gritsan and M. S. Platz, *Chem. Rev.*, 2006, **106**, 3844.
6 H. Bock and R. Dammel, *Angew. Chem., Int. Ed.*, 1987, **26**, 504.
7 E. A. Pritchina, N. P. Gritsan, A. Maltsev, T. Bally, T. Autrey, Y. Liu, Y. Wang and J. P. Toscano, *Phys. Chem. Chem. Phys.*, 2003, **5**, 1010.
8 C. Buron and M. S. Platz, *Org. Lett.*, 2003, **5**, 3383.
9 J. Liu, J. L. Mandel, C. M. Hadad, M. S. Platz, *J. Org. Chem.*, 2004, **69**, 8583.
10 J. Kubicki, Y. Zhang, S. Vyas, G. Burdzinski, H. L. Luk, J. Wang, J. Xue, H. -L. Peng, E. A. Pritchina, M. Sliwa, G. Buntinx, N. P. Gritsan, C. M. Hadad and M. S. Platz, *J. Am. Chem. Soc.*, 2011, **133**, 9751.
11 E. A. Pritchina, N. P. Gritsan and T. Bally, *Russ. Chem. Bull., Int. Ed.*, 2005, **54**, 519.
12 S. Vyas, J. Kubicki, H. L. Luk, Y. Zhang, N. P. Gritsan, C. M. Hadad and M. S. Platz, *J. Phys. Org. Chem.*, 2012, **25**, 693.
13 X. Q. Zeng, H. Beckers, H. Willner, D. Grote and W. Sander, *Chem. Eur. J.*, **2011**, *17*, 3977.
14 J. Kubicki, Y. Zhang, J. Wang, H. L. Luk, H.-L. Peng, S. Vyas and M. S. Platz, *J. Am. Chem. Soc.*, 2009, **131**, 4212.
15 M. P. Sherman and W. S. Jenks, *J. Org. Chem.*, 2014, **79**, 8977.
16 X. Q. Zeng, H. Beckers, H. Willner, P. Neuhaus, D. Grote and W. Sander, *Chem. Eur. J.*, 2009, **15**, 13466.
17 R. D. McCulla, G. A. Gohar, C. M. Hadad and M. S. Platz, *J. Org. Chem.*, 2007, **72**, 9426.
18 G. A. Gohar and M. S. Platz, *J. Phys. Chem. A*, 2003, **107**, 3704.
19 X. Q. Zeng, H. Beckers, P. Neuhaus, D. Grote and W. Sander, *Z. Anorg. Allg. Chem.*, 2012, **638**, 526.
20 X. Q. Zeng, H. Beckers and H. Willner, *J. Am. Chem. Soc.*, 2013, **135**, 2096.
21 J. Kubicki, H. L. Luk, Y. Zhang, S. Vyas, H. -L. Peng, C. M. Hadad and M. S. Platz, *J. Am. Chem. Soc.*, 2012, **134**, 7036.
22 V. Desikan, Y. Liu, J. P. Toscano and W. S. Jenks, *J. Org. Chem.*, 2008, **73**, 4398.
23 X. Q. Zeng, H. Beckers and H. Willner, *J. Am. Chem. Soc.*, 2011, **133**, 20696.
24 X. Q. Zeng, H. Beckers and H. Willner, *Angew. Chem., Int. Ed.*, 2011, **50**, 482.
25 X. Q. Zeng, H. Beckers, H. Willner and J. F. Stanton, *Angew. Chem., Int. Ed.*, 2011, **50**, 1720.
26 X. Q. Zeng, H. Beckers, H. Willner and J. F. Stanton, *Eur. J. Inorg. Chem.*, 2012, 3403.
27 C. J. Shaffer and D. Schröder, *Angew. Chem., Int. Ed.*, 2011, **50**, 2677.
28 S. R. O'Neill and J. M. Shreeve, *Inorg. Chem.*, 1972, **11**, 1629.
29 H. G. Schnöckel and H. Willner, *Infrared and Raman Spectroscopy, Methods and Applications*, VCH: Weinheim, 1994.
30 M. Griffin, A. Muys, C. Noble, D. Wang, C. Eldershaw, K. E. Gates, K. Burrage and G. R. Hanson, *Mol. Phys. Rep.*, 1999, **26**, 60.
31 A. D. Becke, *J. Chem. Phys.*, 1993, **98**, 5648.
32 J. P. Perdew, *Phys. Rev. B*, 1986, **33**, 8822.
33 C. Adamo, V. Barone, *J. Chem. Phys.*, 1998, **108**, 664.
34 J. A. Montgomery, M. J. Frisch, J. W. Ochterski and G. A. Petersson, *J. Chem. Phys.*, 2000, **112,** 6532.
35 C. Gonzalez and H. B. Schlegel, *J. Chem. Phys.*, 1989, **90**, 2154.
36 C. Gonzalez and H. B. Schlegel, *J. Phys. Chem.*, 1990, **94**, 5523.
37 M. J. Frisch, G. W. Trucks, H. B. Schlegel, G. E. Scuseria, M. A. Robb, J. R. Cheeseman, J. A. Montgomery, T. Vreven, K. N. Kudin, J. C. Burant, J. M. Millam, S. S. Iyengar, J. Tomasi, V. Barone, B. Mennucci, M. Cossi, G. Scalmani, N. Rega, G. A. Petersson, H. Nakatsuji, M. Hada, M. Ehara, K. Toyota, R. Fukuda, J. Hasegawa, M. Ishida, T. Nakajima, Y. Honda, O. Kitao, H. Nakai, M. Klene, X. Li, J. E. Knox, H. P. Hratchian, J. B. Cross, C. Adamo, J. Jaramillo, R. Gomperts, R. E. Stratmann, O. Yazyev, A. J. Austin, R. Cammi, C. Pomelli, J. W. Ochterski, P. Y. Ayala, K. Morokuma, G. A. Voth, P. Salvador, J. J. Dannenberg, V. G. Zakrzewski, S. Dapprich, A. D. Daniels, M. C. Strain, O. Farkas, D. K. Malick, A. D. Rabuck, K. Raghavachari, J. B. Foresman, J. V. Ortiz, Q. Cui, A. G. Baboul, S. Clifford, J. Cioslowski, B. B. Stefanov, G. Liu, A. Liashenko, P. Piskorz, I. Komaromi, R. L. Martin, D. J. Fox, T. Keith, M. A. Al-Laham, C. Y. Peng, A. Nanayakkara, M. Challacombe, P. M. W. Gill, B. Johnson, W. Chen, M. W. Wong, C. Gonzalez and J. A. Pople, *Gaussian 03, Revision D.01*, Gaussian, Inc., Pittsburgh PA, 2003.
38 R. Ahlrichs, R. Becherer, M. Binnewies, H. Borrmann, M. Lakenbrink, S. Schunck and H. Schnöckel, *J. Am. Chem. Soc.*, 1986, 108, 7905.
39 M. Houser, S. Kelley, V. Maloney, M. Marlow, K. Steininger and H. Zhou, *J. Phys. Chem.*, 1995, **99**, 7946.
40 B. Gatehouse, T. Brupbacher and M. C. L. Gerry, *J. Phys. Chem. A*, 1999, **103**, 560.
41 H. Beckers, H. Bürger, P. Paplewski, M. Bogey, J. Demaison, P. Dréan, A. Walters, J. Breidung and W. Thiel, *Phys. Chem. Chem. Phys.*, 2001, **3**, 4247.
42 X. Q. Zeng, M. Gerken, H. Beckers and H. Willner, *Inorg. Chem.* 2010, **49**, 3002.
43 S. Vyas, S. Muthukrishnan, J. Kubicki, R. D. McCulla, G. Burdzinski, M. Sliwa, M. S. Platz and C. M. Hadad, *J. Am. Chem. Soc.*, 2010, **132**, 16796.
44 A. A. Korkin, P. von R. Schleyer and R. J. Boyd, *Chem. Phys. Lett.*, 1994, **227**, 312.
45 C. J. Shaffer, B. J. Esselman, R. J. McMahon, J. F. Stanton, R. C. Woods, *J. Org. Chem.*, 2010, **75**, 1815.